THE JOURNAL OF PHYSICAL CHEMISTRY C

pubs.acs.org/JPCC Article

Surface Reconstruction, Hydration, and Adhesion of Epoxy to the (0001) Surface of α-Berlinite: Insights from Density Functional Theory Calculations

Espen Sagvolden, Martin F. Sunding, and Ole Swang*

Cite This: *J. Phys. Chem. C* 2020, 124, 6683−6688 Read Online

ACCESS | Metrics & More | Article Recommendations | Supporting Information

ABSTRACT: Phosphoric acid anodization (PAA) is a candidate for replacement of toxic chromates during the surface treatment of aluminum prior to gluing in the aerospace industry. During PAA, a layer of $AlPO_4$ forms on top of the alumina layer. We apply density functional theory computations to investigate how the $AlPO_4$ surface reorganizes and how it bonds to water and adhesives. As our $AlPO_4$ model, we use the α-berlinite (0001) surface. Taking the structure of the α-quartz (0001) surface reported by Rignanese et al. (Rignanese, G.-M.; De Vita, A.; Charlier, J.-C.; Gonze, X.; Car, R., *Phys. Rev. B* 2000, *61*, 13250−13255) as a starting point, we find that the α-berlinite surface reconstructs. The lowest energy structure for α-berlinite (0001) is found to have a buckled configuration, with three-coordinated phosphorus protruding out of the surface and a neighboring aluminum atom binding to five oxygens. Different structures for the hydrated surface $AlPO_4{\cdot}0.25H_2O$ are presented, of which the most stable involves hydroxylation of the aforementioned buckle and of a new phosphorus buckle, accompanied by formation of a P−Al dative bond. We report results for the adhesion of a glue fragment derived from bisphenol A to the surface. The lowest energy is found for a covalently bonded structure, mimicking the most stable hydroxylated structure. The adhesion energy of the glue increases strongly when it is covalently bonded to the surface rather than being hydrogen bonded, providing superior adhesion to the material.

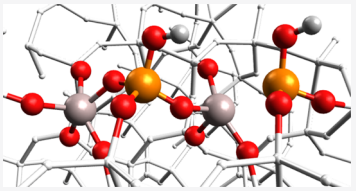

INTRODUCTION

Adhesion is a phenomenon of great importance for applications in joining and coating, at least in the automotive and aerospace industries. In the race to minimize weight and fuel consumption, adhesive bonding is important since it facilitates fiber−metal laminates[1] and bonding of components, which are difficult to join by other techniques (*e.g.*, joining of aluminum with steel, polymers, or composites). Furthermore, as opposed to attachments using screws, bolts, or rivets, glued joints weigh less and provide a uniform force distribution. Equally important is the use of adhesives as protective (anti-corrosive) and decorative paint on surfaces.

The exact mechanism of adhesion seems to be debated, with two theories dominating. One theory being that the adhesive force comes from interlocking created when the adhesive fills pores on the substrate before solidifying.[2−5] The other theory being that atomic scale interactions (*e.g.*, hydrogen bonds or electrostatic interactions) between the substrate and the coating/glue account for the adhesion.[6−10] Recent research indicates that both mechanisms contribute to adhesion.[11] In the present contribution, we are concerned exclusively with the atomic scale interactions.

Aluminum is a material of special interest to the aerospace industry and, increasingly, to the automotive industry. Upon exposure to air, aluminum will quickly react and form an Al_2O_3 surface layer,[12] which lends some protection against further corrosion. However, this layer is insufficient to protect against corrosion for many applications. To improve corrosion resistance, it is advantageous to replace the thin oxide layer with an impenetrable barrier layer. On the other hand, for maximum interlocking and bonding with a subsequently applied coating or adhesive, a rough and porous surface is beneficial. To simultaneously address both requirements, aluminum is invariably pre-treated prior to gluing or coating.

Industrial processes exist to achieve a surface with an impenetrable layer on the bottom and a porous structure on top. The aluminum surface is electrochemically oxidized in the presence of an acid (anodization). The properties of the anodization layer depend, among other things, on the choice of acid. Chromic acid anodization (CAA), using hexavalent chromium, has been widely used in the aerospace industry, since it produces a layer with both excellent corrosion resistance and bonding properties. However, since chromates are carcinogenic and pose occupational and public health risks,[13] they will likely be banned in the future. Significant effort has been put into investigating alternative anodization techniques using more environmentally benign acids: phosphoric acid anodization (PAA), sulfuric acid anodization (SAA), phosphoric−sulfuric acid anodization (PSA), boric−

Received: December 20, 2019
Revised: March 2, 2020
Published: March 3, 2020

https://dx.doi.org/10.1021/acs.jpcc.9b11794
J. Phys. Chem. C 2020, 124, 6683−6688

sulfuric acid anodization, and tartaric−sulfuric acid anodization have been reported,[14] as have sol−gel approaches.[15,16] Our present interest concerns PAA aluminum.

Knaup et al.,[17] using semiempirical density functional-based tight binding (DFTB) calculations, studied the adhesion of (among others) the unreacted diglycidylether of bisphenol A (DGEBA) (Figure 1a) to native alumina. They reported

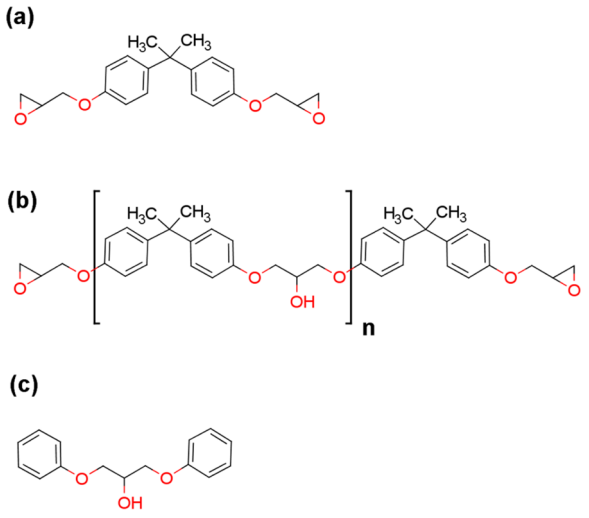

Figure 1. (a) DGEBA molecule. (b) Prepolymerization of DGEBA with BPA, providing a resin. (c) 1,3-bis(phenoxy)propan-2-ol molecule used as a model for epoxy glue.

formation of covalent bonds between adhesives and the surface. While DGEBA has two epoxide groups, prepolymerization of DGEBA with bisphenol-A (BPA) will create oligomers as shown in Figure 1b. Bonding of this type of epoxy resin to hydroxylated γ-alumina surfaces has been studied at the DFT level of theory by Semoto et al.[18] They modeled epoxy resin as epoxy oligomers (Figure 1b) or a single molecule of 1,3-bis(phenoxy)propan-2-ol (BPP) (Figure 1c). Only hydrogen bonding between epoxy−resin hydroxyl groups and alumina was considered.

It has been experimentally verified by Davis et al.[19] that the surface of PAA aluminum consists of alumina covered by a layer of $AlPO_4$. Abrahami et al.[20] confirmed this and found that this is also the case for PSA aluminum. Davis et al.[19] reported that their samples were covered by a monolayer of $AlPO_4$, but that the thickness depended on production conditions, such as the choice of rinsing fluid. To determine whether an $AlPO_4$ surface is the appropriate atomic scale model for PAA aluminum, we have analyzed the XPS data from ref 20, and find that their PAA-treated aluminum surfaces appear to be covered by a 2−2.5 nm-thick layer of $AlPO_4$ on top of the alumina layer, while PSA-treated aluminum shows a thinner layer (see the Supporting Information). Hence, we feel confident that for studies of bonding or painting of PAA or PSA aluminum, the relevant surface is that of $AlPO_4$. We are not aware of any other experimental, atomic scale characterization of PAA aluminum surfaces. XANES, FTIR (DRIFTS), or other surface-specific spectroscopic results would have been helpful; as it is, we had to choose rather arbitrarily what surface to use as a model and settled for the α-berlinite (0001) surface.

In the present work, we have investigated the structure of the α-berlinite (0001) surface, its hydration, and the adhesion of epoxy adhesives derived from BPA to it as a model for adhesion to PAA-treated aluminum surfaces. Water adhesion is not only studied for the importance of hydration energies but also because water bonding is an excellent prototype for the bonding of the OH groups of the epoxy resin to $AlPO_4$. The questions to be addressed by the paper are: what is the structure of the reorganized (0001) surface of α-berlinite? How does it hydrate, by hydrogen bonding or by hydroxylation, and at which sites? And finally, does BPP bond covalently or by hydrogen bonding, and which bonding sites are preferred? Our paper is organized as follows: the Computational Details are presented in the next section followed by a combined Results and Discussion section, and finally, Conclusions.

COMPUTATIONAL DETAILS

We are unaware of prior computational studies of the α-berlinite (0001) surface. However, α-berlinite is isostructural to α-quartz, with the Si atoms substituted by Al and P. Several computational studies of the α-quartz (0001) surface exist.[21−23] Rignanese et al.[21] explored several reorganizations for the α-quartz (0001) surface and found that the structure that they termed the dense model (Figure 5 in their paper) had the lowest energy. This structure involves a reorganization in which the upper layer Si atoms sinks into the next layer of Si atoms, resulting in six-membered rings on the surface.

Starting from the α-berlinite structure reported by Muraoka and Kihara,[24] we optimized the bulk structure after testing for the k-point and basis set convergence (vide infra). A 2 × 2 × 1 supercell of the resulting structure is illustrated in Figure 2. To

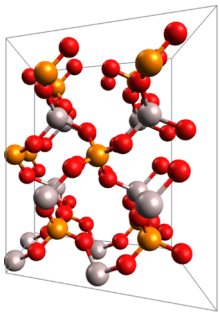

Figure 2. Structure of α-berlinite (0001). Illustrated is a 2 × 2 × 1 supercell. Color codes: P (orange), Al (light gray), and O (red).

create the analog of the dense α-quartz structure, we created a slab by cleaving the α-berlinite in the (0001) direction and inserting a 20 Å vacuum. Hence, the slab is one unit cell thick, comprising three layers each of P and Al; slabs of other thicknesses have not been investigated here. Cell parameters and the positions of the lowest layer of Al and lowest layer of P were then frozen for all subsequent computations; all other fractional coordinates were optimized throughout.

Subsequent to cleaving, we constructed and relaxed the dense surface structure equivalent to that reported by Rignanese et al.[21] for quartz and investigated further the lower-lying surface reorganizations using 2 × 2, 3 × 3, and 4 × 4 surface super cells. To study surface hydration, we studied water bonding sites on the reconstructed 2 × 2 surface unit cell. Both hydrogen bonding of intact water molecules to the surface and water dissociation followed by hydroxylation were considered. Regarding water as a prototype of the bonding of the OH group of BPP to the surface, we investigated resin−

https://dx.doi.org/10.1021/acs.jpcc.9b11794
J. Phys. Chem. C 2020, 124, 6683−6688

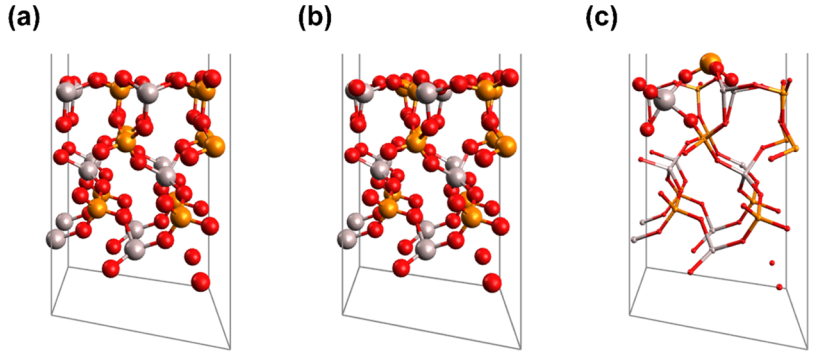

Figure 3. Reorganized structures of the α-berlinite (0001) surface. (a) Dense A structure corresponding to the dense structure of α-quartz. (b) Slightly symmetry-broken and more stable Dense B structure. (c) Buckled structure. In panel (c), only atoms participating in the buckle are highlighted as balls. Color codes: P (orange), Al (light gray), and O (red).

berlinite structures mimicking the most energetically promising hydration structures. Because of the size of BPP, the latter study was conducted in a 4 × 4 surface unit cell.

All computations were performed using the density functional theory and a plane−wave basis using VASP 5.4.4. The PBE density functional[25] was used with PAW pseudopotentials. We chose hard PAW pseudopotentials for C, H, O, and P where all valence electrons were treated explicitly. For Al, we chose a pseudopotential where all electrons, except 1s electrons, were treated explicitly. All computations were performed using Grimme-D3 van der Waals corrections[26] and Gaussian smearing of the orbital occupation with an energy parameter of 0.2 eV.

We found that choosing a k-point density better than 0.4 $Å^{-1}$ and the plane-wave basis-set cutoff at 1000 eV provided convergence of bulk unit-cell lattice parameters within 0.2% with respect to increasing the cutoff to 1100 eV or the increasing k-point density to better than 0.2 $Å^{-1}$. All reported structures have been computed using these parameters. In 2 × 2 and 3 × 3 surface-cell computations, a k-point density of 0.4 $Å^{-1}$ amounts to a 2 × 2 × 1 k-point grid, while in computations involving a 4 × 4 surface cell, it amounts to a gamma-point computation. All structures were optimized to the point where no residual forces exceeded 10^{-3} eV/Å.

From all converged structures, energies were computed in two single-point computations with basis set cutoffs of 1000 and 1100 eV to further assure convergence. Dipole and quadrupole interactions between repeat images in the z-direction were eliminated by extrapolating to infinite separation (see input files in the Supporting Information for exact choice of keywords). Relative to a basis set cutoff of 1100 eV, it was found that both total and relative energies were converged to within 0.01 eV at a basis set cutoff of 1000 eV. Reported relative energies are electronic energies.

RESULTS AND DISCUSSION

α-Berlinite (0001) Surface. After cleaving, we constructed the dense surface found by Rignanese et al.[21] for α-quartz and relaxed the structure to a stable structure similar to the α-quartz dense structure. In the following, this structure will be called Dense A. We also found another minimum, a slightly symmetry-broken reconstructed structure (Dense B), with an energy 0.3 eV lower (per 2 × 2 surface cells) than that of Dense A.

However, we also found a third buckled structure with 2.3 eV lower energy than Dense A per 2 × 2 surface cell. This structure, which was found after the first structures with adsorbed water was investigated, is characterized by a protruding phosphorus atom bound in a pyramidal fashion to three oxygen atoms and a neighboring aluminum atom that sinks into the surface, binding to five oxygens. Five-coordinated aluminum is known from the inner surfaces of porous aluminum phosphates.[27] The three structures are shown in Figure 3.

To elucidate the optimal buckle density, we also investigated the energy of formation of one buckle per 3 × 3 and one per 4 × 4 surface cell (buckle-formation energies found by comparing to 3 × 3 and 4 × 4 cells in the Dense A structure). We found that the energy per buckle is even higher at lower densities, with a buckle-formation energy as high as 5.3 eV in the 4 × 4 surface cell. However, in terms of energy per formula unit, forming one buckle per 2 × 2 cell is advantageous (0.6 eV) compared to one per 3 × 3 (0.5 eV) or 4 × 4 (0.3 eV); see Table 1.

Table 1. Energy of Surface Structures Relative to the Dense A Structure ($E_{rel} = E_{buckled} - E_{DenseA}$)[a]

energy	2 × 2 Dense B	2 × 2 buckled	3 × 3 buckled	4 × 4 buckled
E_{rel} (eV)	−0.3	−2.3	−4.6	−5.3
E_{rel} (eV per formula unit)	−0.1	−0.6	−0.5	−0.3

[a]All energies are in eV.

Hydration of the Berlinite Surface. We investigated hydrogen bonding and hydroxylation formed by one water molecule and the 2 × 2 buckled surface cell. Three hydroxylated structures (Figure 4) were considered, with OH on, respectively, (a) two P, (b) one P and one Al, and (c) two Al. An additional O must be taken from the surface to form the hydroxyls. In the void left by the oxygen, we observe the formation of an Al−P bond. The Al−P bond may be understood as a Lewis acid−base reaction between P (lone pair donor) and Al (acceptor), hence forming a dative bond.

Of the hydroxylated structures, only the structure with OH on two P (Figure 4 a) is stable with respect to water vapor and the dry berlinite surface. This is also by far the most stable of all investigated hydrated structures, with a water adsorption energy of 1.3 eV. In this structure, an additional buckle is formed by the dative bonded P. Also, the dative bonded Al is bound to four O in addition to P. In addition, the original P buckle and five-coordinated Al from the dry buckled surface

https://dx.doi.org/10.1021/acs.jpcc.9b11794
J. Phys. Chem. C 2020, 124, 6683−6688

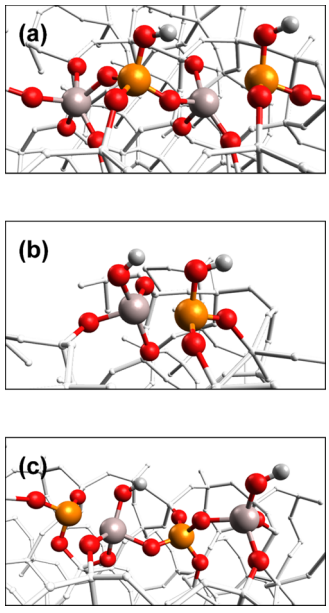

Figure 4. Hydroxylated structures with OH groups on (a) two P, (b) neighboring Al and P, and (c) two Al. Al−P dative bonds arise as an O is ejected from the bulk structure to form the surface hydroxyls. Color codes: P (orange), Al (large light gray balls), H (small light gray balls), and O (red).

remain. The hydroxyls bind covalently to the two P buckles. The energies and Al−P dative bond length are displayed in Table 2.

Table 2. Hydration Energies E_{hyd} = E(product) − E(reactants) of the Hydrated Structures (eV)[a]

hydrated structure	E_{hyd} (eV)	Al−P bond length (Å)
4(a)	−1.3	2.58
4(b)	0.7	2.52
4(c)	0.6	2.50
6(a)	−0.4	
6(b)	−0.4	
6(c)	−0.2	

[a]Here, the reactant would be a gas-phase water molecule and the buckled dry surface with one buckle per 2 × 2 surface super cell, while the product involves two hydroxyl groups formed by dissociative chemisorption of water on the surface. Also given is the length of the Al−P dative bond formed in the hydroxylated structures.

While we have not computed reaction pathways and barriers, this structure was found serendipitously while optimizing a qualitatively different structure, which relaxed into this minimum. This should indicate that barriers are low. Details of this structure, the dative interaction showing more clearly, are illustrated in Figure 5.

In Figure 6, we display the three most promising hydrogen-bonded structures. Hydrogen bonding to either of the four-coordinated surface Al provides energies 0.2−0.4 eV lower than that of the free species. We found no stable structures involving hydrogen bonds between water and P or five-coordinated Al.

Bond lengths in the P buckle of pristine α-berlinite (0001) when there is one buckle per 2 × 2 and 4 × 4 surface supercells are displayed in Figure 7. In addition, we display the bond

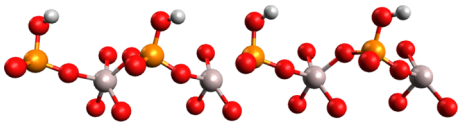

Figure 5. Details of the hydroxylated moiety of Figure 4a. When using a 2 × 2 super cell, what arises is a ridge alternating between dative-bonded buckles and the buckles found on the dry surface. Color codes: P (orange), Al (large light gray balls), H (small light gray balls), and O (red).

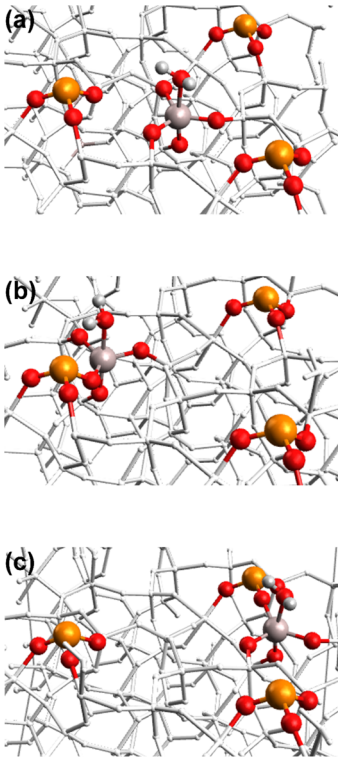

Figure 6. Hydrogen bonding sites for water on the berlinite (0001) surface: (a) on Al not adjacent to a buckle, (b) on an Al adjacent to the depressed side of a buckle, and (c) on Al adjacent to the elevated side of the buckle. Color codes: P (orange), Al (large light gray balls), H (small light gray balls), and O (red).

lengths in the same pyramid after hydroxylation in the lowest-energy hydration structure.

We see clearly that the P−O bonds become shorter when there is an OH group attached to the buckle. This can be understood through the valence theory: without a hydroxyl group, P has a lone pair and forms a single bond to each of its

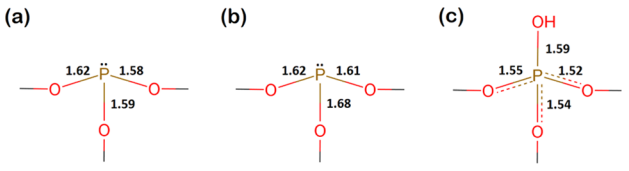

Figure 7. Bond lengths (in Å) at the phosphorus buckle: (a) as calculated in a 2 × 2 super cell, (b) as calculated for a lone buckle on a 4 × 4 super cell, and (c) hydroxylated buckle in structure where only P is hydroxylated (computed using a 2 × 2 super cell). In the latter case, one electron from the former lone pair becomes available for bonding to the oxygens, and we observe a corresponding shortening of the bond lengths.

https://dx.doi.org/10.1021/acs.jpcc.9b11794
J. Phys. Chem. C 2020, 124, 6683−6688

three O. When the hydroxyl binds to the site of the lone pair, an electron is freed up, and a double bond can be formed to any of the oxygens. Assuming that this is a resonance structure, all three P−O bonds may be assigned a bond order of 4/3. The increased bond lengths in the buckle in the 4 × 4 surface cell are probably due to relaxation effects. Given the much lower energy per buckle in the 4 × 4 cell, it is reasonable to expect a fair amount of structural relaxation.

BPP Surface Adhesion. Under the assumption that the most favorable hydration scenarios should also be the most favorable scenarios for binding the OH group of BPP to the surface, we investigated the three, assumedly most favorable, scenarios for the interaction between an epoxy coating and the surface. The structures can be found in Figure 8 and energies in Table 3. All three structures provide bonding. The hydrogen-bonded structures have an adhesion energy of 1.2−1.3 eV, versus 2.1 eV for the covalently bonded structure corresponding to the hydroxylated structure in Figure 4a. Thus, the difference in adhesion energy between covalently bonded, and hydrogen-bonded structures remains approximately the same as in hydration.

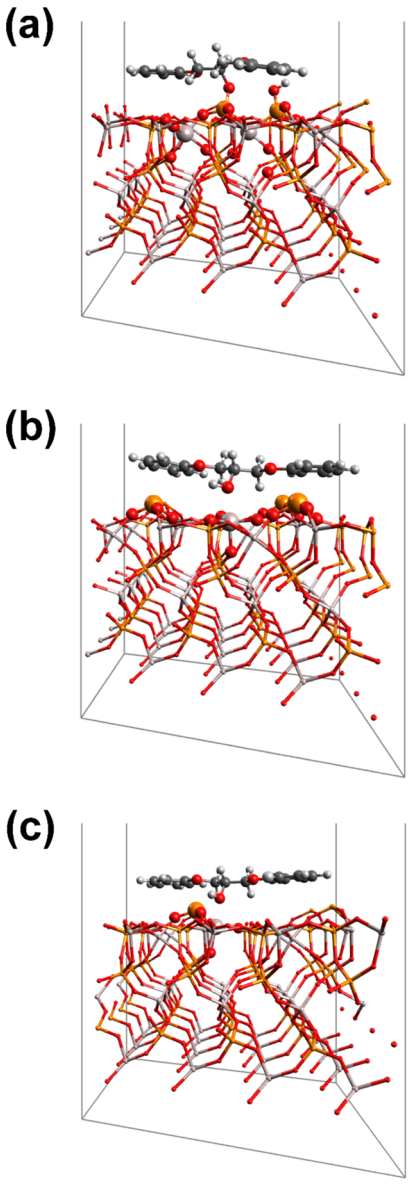

Figure 8. Structures of adhered BPP. (a) Covalently bonded structure. (b) Hydrogen-bonded structure at Al far from buckles. (c) Hydrogen-bonded structure at Al at the low side of a buckle. Color codes: P (orange), Al (large light gray balls), H (small light gray balls), C (dark gray), and O (red).

Table 3. Adhesion Energy Change of Three Investigated Energy Minima for BPP Adhesion to Surface (eV)[a]

structure	$E_{adhesion}$ (eV)
8(a)	−2.1
8(b)	−1.2
8(c)	−1.3

[a]The covalently bonded structure is 0.8−0.9 eV more energetically stable than the hydrogen-bonded structures.

CONCLUSIONS

We report the first DFT study of the α-berlinite (0001) surface and have found that it does not reorganize to the dense structure as the corresponding α-quartz surface does but rather to a structure containing P bound to only three O in a pyramidal buckle next to an Al bound to five O. The optimal density of such buckles appears to be of the order of one buckle per four surface P atoms. The buckled surface structure of α-berlinite (0001) has not, to our knowledge, been reported earlier. Also, no similar structures appear to have been found for α-quartz. The latter is not surprising, since a pure silicon oxide like α-quartz will have less local polarization compared to the corresponding aluminum phosphate.

In the present work, we have investigated the hydration $AlPO_4{\cdot}0.25H_2O$, and it appears to take place by hydroxylation of two phosphorus atoms. Both hydroxylated phosphorus atoms form pyramidal buckles with oxygen, one of which is the buckle retained from the unhydrated surface, while the other is facilitated by formation of a dative bond with aluminum.

We have also investigated bonding of BPP, as a proxy for BPA-based epoxy adhesive, to a completely dry α-berlinite (0001) surface. The assumed bonding moieties of the adhesive are the hydroxyl groups, and the hydroxyl group of the BPP appears to form covalent bonds to $AlPO_4$; we note the strong similarity between the mechanisms of bonding between the two adsorbates. The covalently bonded structure is much more stable than the hydrogen-bonded species. Dry berlinite surfaces could possibly be attained by heating in a dry atmosphere. However, given the water affinity of $AlPO_4$, it would be highly interesting, especially from an application point of view, to complement the current study with a study of the reaction of glue to hydrated berlinite.

ASSOCIATED CONTENT

Supporting Information

The Supporting Information is available free of charge at https://pubs.acs.org/doi/10.1021/acs.jpcc.9b11794.

Details on the analysis of XPS results, VASP input files (INCAR) for structural optimization and single-point computations, and list of PAW pseudopotential (POTCAR) files used in the computations. (PDF)

cif files of all reported converged structures; relative to the provided cif-files, some figures in the article may have been translated for improved clarity; for ease of reference, the individual cif files are named after the corresponding figure or have been given a descriptive name (ZIP)

https://dx.doi.org/10.1021/acs.jpcc.9b11794
J. Phys. Chem. C 2020, 124, 6683−6688

AUTHOR INFORMATION

Corresponding Author

Ole Swang − *SINTEF, Process Technology, Oslo N-0314, Norway;* orcid.org/0000-0002-8550-0084; Phone: +47 98 24 39 34; Email: ole.swang@sintef.no

Authors

Espen Sagvolden − *SINTEF, Sustainable Energy Technology, Oslo N-0314, Norway*

Martin F. Sunding − *SINTEF, Sustainable Energy Technology, Oslo N-0314, Norway*

Complete contact information is available at: https://pubs.acs.org/10.1021/acs.jpcc.9b11794

Author Contributions

The manuscript was written through contributions of all authors. All authors have given approval to the final version of the manuscript.

Notes

The authors declare no competing financial interest.

ACKNOWLEDGMENTS

The authors gratefully acknowledge funding from the Research Council of Norway under grant no. 194068 and a generous grant of computing resources from the Research Council of Norway under the Sigma2 program account nos. NN2147k and NN9393k. Figures 1 and 7 have been prepared with the help of MarvinSketch 19.24 provided free by ChemAxon.

ABBREVIATIONS

DFT density functional theory; DFTB density functional-based tight binding; DGEBA diglycidyl ether of bisphenol-A; BPA bisphenol-A; BPP 1,3-bis(phenoxy)propan-2-ol; PAA phosphoric acid anodization; CAA chromic acid anodization; SAA sulfuric acid anodization; PSA phosphoric−sulfuric acid anodization

REFERENCES

(1) Straznicky, P. V.; Laliberté, J. F.; Poon, C.; Fahr, A. Applications of Fiber-Metal Laminates. *Polym. Compos.* **2000**, *21*, 558−567.

(2) Venables, J. D.; McNamara, D. K.; Chen, J. M.; Sun, T. S.; Hopping, R. L. Oxide Morphologies on Aluminum Prepared for Adhesive Bonding. *Appl. Surf. Sci.* **1979**, *3*, 88−98.

(3) Packham, D. E. Surface Energy, Surface Topography and Adhesion. *Int. J. Adhes. Adhes.* **2003**, *23*, 437−448.

(4) Packham, D. E.; Johnston, C. Mechanical Adhesion: were McBain and Hopkins Right? An Empirical Study. *Int. J. Adhes. Adhes.* **1994**, *14*, 131−135.

(5) Allen, K. W. Some Reflections on Contemporary Views of Theories of Adhesion. *Int. J. Adhes. Adhes.* **1993**, *13*, 67−72.

(6) van den Brand, J.; Blajiev, O.; Beentjes, P. C. J.; Terryn, H.; de Wit, J. H. W. Interaction of Anhydride and Carboxylic Acid Compounds with Aluminum Oxide Surfaces Studied Using Infrared Reflection Absorption Spectroscopy. *Langmuir* **2004**, *20*, 6308−6317.

(7) Abrahami, S. T.; Hauffman, T.; de Kok, J. M. M.; Mol, J. M. C.; Terryn, H. Effect of Anodic Aluminum Oxide Chemistry on Adhesive Bonding of Epoxy. *J. Phys. Chem. C* **2016**, *120*, 19670−19677.

(8) van den Brand, J.; Blajiev, O.; Beentjes, P. C. J.; Terryn, H.; de Wit, J. H. W. Interaction of Ester Functional Groups with Aluminum Oxide Surfaces Studied Using Infrared Reflection Absorption Spectroscopy. *Langmuir* **2004**, *20*, 6318−6326.

(9) Özkanat, Ö.; Salgin, B.; Rohwerder, M.; de Wit, J. H. W.; Mol, J. M. C.; Terryn, H. Interactions at Polymer/(oxyhydr)oxide/aluminium Interfaces Studied by Scanning Kelvin Probe. *Surf. Interface Anal.* **2012**, *44*, 1059−1062.

(10) Abrahami, S. T.; Hauffman, T.; de Kok, J. M. M.; Terryn, H.; Mol, J. M. C. The Role of Acid-Base Properties in the Interactions across the Oxide-Primer Interface in Aerospace Applications. *Surf. Interface Anal.* **2016**, *48*, 712−720.

(11) Abrahami, S. T.; de Kok, J. M. M.; Gudla, V. C.; Ambat, R.; Terryn, H.; Mol, J. M. C. Interface Strength and Degradation of Adhesively Bonded Porous Aluminum Oxides. *npj Mater. Degrad.* **2017**, *1*, 1−8.

(12) Batra, I. P.; Kleinman, L. Chemisorption of Oxygen on Aluminum Surfaces. *J. Electron Spectrosc. Relat. Phenom.* **1984**, *33*, 175−241.

(13) Salnikow, K.; Zhitkovich, A. Genetic and Epigenetic Mechanisms in Metal Carcinogenesis and Cocarcinogenesis: Nickel, Arsenic, and Chromium. *Chem. Res. Toxicol.* **2008**, *21*, 28−44.

(14) García-Rubio, M.; de Lara, M. P.; Ocón, P.; Diekhoff, S.; Beneke, M.; Lavía, A.; García, I. Effect of postreatment on the corrosion behaviour of tartaric−sulphuric anodic films. *Electrochim. Acta* **2009**, *54*, 4789−4800.

(15) Meyer, S.; Schubert, U.; De Bardi, M.; Wiesinger, R.; Schreiner, M.; Grohmann, T. Adhesion Pretreatment of Aluminum by Sol−Gel Processing. *Int. J. Adhes. Adhes.* **2014**, *51*, 103−110.

(16) Costenaro, H.; Lanzutti, A.; Paint, Y.; Fedrizzi, L.; Terada, M.; de Melo, H. G.; Olivier, M.-G. Corrosion Resistance of 2524 Al Alloy Anodized in Tartaric-Sulphuric Acid at Different Voltages and Protected with a TEOS-GPTMS Hybrid Sol-Gel Coating. *Surf. Coat. Technol.* **2017**, *324*, 438−450.

(17) Knaup, J. M.; Köhler, C.; Frauenheim, T.; Blumenau, A. T.; Amkreutz, M.; Schiffels, P.; Schneider, B.; Hennemann, O.-D. Computational Studies on Polymer Adhesion at the Surface of γ-Al2O3. I. The Adsorption of Adhesive Component Molecules from the Gas Phase. *J. Phys. Chem. B* **2006**, *110*, 20460−20468.

(18) Semoto, T.; Tsuji, Y.; Yoshizawa, K. Molecular Understanding of the Adhesive Force between a Metal Oxide Surface and an Epoxy Resin. *J. Phys. Chem. C* **2011**, *115*, 11701−11708.

(19) Davis, G. D.; Sun, T. S.; Ahearn, J. S.; Venables, J. D. Application of Surface Behaviour Diagrams to the Study of Hydration of Phosphoric Acid-Anodized Aluminium. *J. Mater. Sci.* **1982**, *17*, 1807−1818.

(20) Abrahami, S. T.; Hauffman, T.; de Kok, J. M. M.; Mol, J. M. C.; Terryn, H. XPS Analysis of the Surface Chemistry and Interfacial Bonding of Barrier-Type Cr(VI)-Free Anodic Oxides. *J. Phys. Chem. C* **2015**, *119*, 19967−19975.

(21) Rignanese, G.-M.; De Vita, A.; Charlier, J.-C.; Gonze, X.; Car, R. First-principles molecular-dynamics study of the (0001) α−quartz surface. *Phys. Rev. B* **2000**, *61*, 13250−13255.

(22) Koudriachova, M. V.; Beckers, J. V. L.; de Leeuw, S. W. Computer Simulation of the Quartz Surface: a Combined Ab Initio and Empirical Potential Approach. *Comput. Mater. Sci.* **2001**, *20*, 381−386.

(23) Chen, Y.-W.; Cao, C.; Cheng, H.-P. Finding Stable α-quartz (0001) Surface Structures via Simulations. *Appl. Phys. Lett.* **2008**, *93*, 181911.

(24) Muraoka, Y.; Kihara, K. The Temperature Dependence of the Crystal Structure of Berlinite, a Quartz-type Form of $AlPO_4$. *Phys. Chem. Miner.* **1997**, *24*, 243−253.

(25) Perdew, J. P.; Burke, K.; Ernzerhof, M. Generalized Gradient Approximation Made Simple. *Phys. Rev. Lett.* **1996**, *77*, 3865. Perdew, J. P.; Burke, K.; Ernzerhof, M. Generalized Gradient Approximation Made Simple. *Phys. Rev. Lett.* **1997**, *77*, 1396.

(26) Grimme, S.; Antony, J.; Ehrlich, S.; Krieg, H. A Consistent and Accurate Ab Initio Parametrization of Density Functional Dispersion Correction (DFT-D) for the 94 Elements H-Pu. *J. Chem. Phys.* **2010**, *132*, 154104.

(27) Fjermestad, T.; Svelle, S.; Swang, O. Mechanism of Si Island Formation in SAPO-34. *J. Phys. Chem. C* **2015**, *119*, 2086−2095.